



BNL-225843-2024-TECH

C-A/AP/711

A possible origin of the 10-15% polarization loss observed in RHIC beyond 100 GeV

F. Méot

July 2024

Collider Accelerator Department
Brookhaven National Laboratory

U.S. Department of Energy

USDOE Office of Science (SC), Nuclear Physics (NP)

Notice: This technical note has been authored by employees of Brookhaven Science Associates, LLC under Contract No. DE-SC0012704 with the U.S. Department of Energy. The publisher by accepting the technical note for publication acknowledges that the United States Government retains a non-exclusive, paid-up, irrevocable, worldwide license to publish or reproduce the published form of this technical note, or allow others to do so, for United States Government purposes.

DISCLAIMER

This report was prepared as an account of work sponsored by an agency of the United States Government. Neither the United States Government nor any agency thereof, nor any of their employees, nor any of their contractors, subcontractors, or their employees, makes any warranty, express or implied, or assumes any legal liability or responsibility for the accuracy, completeness, or any third party's use or the results of such use of any information, apparatus, product, or process disclosed, or represents that its use would not infringe privately owned rights. Reference herein to any specific commercial product, process, or service by trade name, trademark, manufacturer, or otherwise, does not necessarily constitute or imply its endorsement, recommendation, or favoring by the United States Government or any agency thereof or its contractors or subcontractors. The views and opinions of authors expressed herein do not necessarily state or reflect those of the United States Government or any agency thereof.

A possible origin of the 10~15% polarization loss observed in RHIC beyond 100 GeV

François Méot
BNL, Upton, NY, USA

*Tech. Note C-A/AP/711
BNL C-AD*

July 16, 2024

Abstract

This Tech. Note summarizes the outcomes of numerical simulations regarding the dependence on random vertical closed orbit of polarization transmission through strong resonances in RHIC.

Contents

1	Introduction	3
2	Conclusion: Polarization vs. Orbit, Recap Graph	4
Appendix		5
A	Working Hypotheses	5
A.1	Spin Resonance Spectrum, Intrinsic	5
A.2	Spin Resonance Spectrum, Integer	5
A.3	Spin Matrix at IP6	7
A.4	RF Settings	7
A.5	Initial Bunch; Phase-Space Motion	8
B	Transmission Versus <i>rms</i> Orbit Excursion, Simulations	9
B.1	Case 393 + Qy	9
B.2	Case 411 - Qy	10

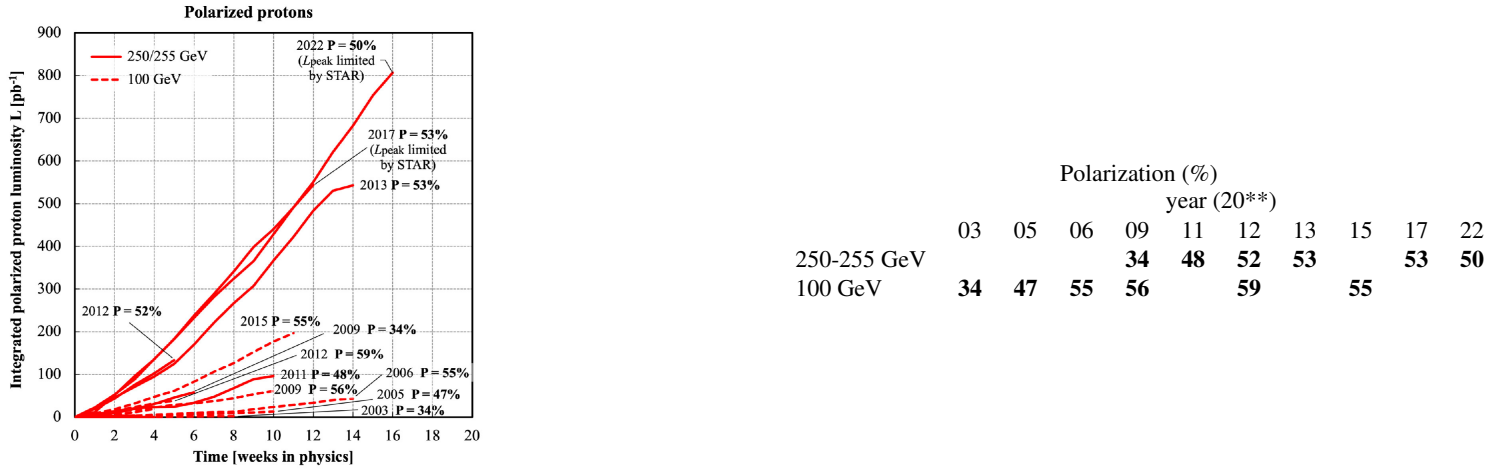
1 Introduction

This Tech. Note summarizes the outcomes of numerical simulation of strong resonance crossing using RHIC lattice, collision optics. The regular RHIC snake configuration is used, *i.e.* 2 snakes at their 3 o'clock and 9 o'clock locations. The working point used is $Q_x/Q_y=28.685/29.673$.

These numerical experiments are performed with, in mind, the 15% polarization loss observed (measured ?) during the ramp between 100 GeV and 255 GeV, and the possibility for the present simulations to point to possible cause(s).

As a matter of fact, it has been stressed in many occasions that it should be checked with simulations how much the vertical orbit would need to be in order to affect polarization. The question has been addressed with SPINK in the past¹, yet it has to be addressed again, following in particular changes on the signs of vertical BPM mechanical offsets which happened in January 2010².

A summary of RHIC polarization data over the years is given below, for the record.



2 Conclusion: Polarization vs. Orbit, Recap Graph

The graph in Fig. 1 summarizes the outcomes of the numerical simulations detailed in Appendix.

Conclusion: a reason for a possible origin for about 10% polarization loss during the ramp beyond 100 GeV, to 250 GeV, appears to just be RHIC's regular closed orbit. The latter has a marginal effect up to and including the intrinsic resonance $411 - Qy \approx 381$ i.e. 200 GeV, but no longer across $393 + Qy \approx 220$ GeV, Fig. 1.

RHIC vertical closed orbit being a possible cause comes as a surprise (to me at least) as one would expect such obvious cause to have long been explored. Regarding the strongest resonance, $393+Qy$: whereas one particular $160 \mu\text{m}$ *rms* random orbit sample in the present crossing simulation only yields a low 3% loss (page 9), moving to twice as much instead, i.e. $320 \mu\text{m}$ *rms* random orbit, yields 24% loss. A 10% polarization loss through $393+Qy$ with the present random orbit sample correlates with a $200 \mu\text{m}$ *rms* defect (Fig. 1).

To bear in mind: different dipole defects (different random seeds) yield different vertical closed orbits and *rms* excursions. These may noticeably differ from each other, and so may the depolarizing effect they result in. Here, we tend to consider that a particular random orbit provides a reasonable estimate of polarization transmission for a particular *rms* orbit excursion. In some cases, two or more different orbits are tracked, as a sanity check regarding the latter hypothesis.

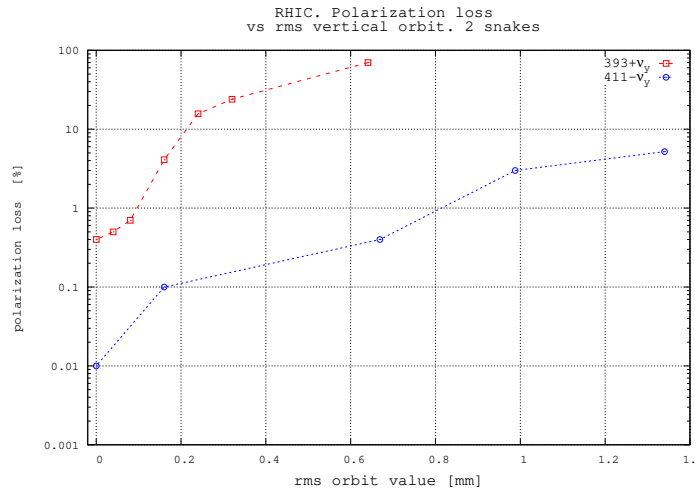


Figure 1: Polarization loss through $411-Qy$ and $393+Qy$ resonances, vs. *rms* closed orbit value. Transverse beam densities are Gaussian, $2.5 \mu\text{m}$ *rms*, momentum spread is Gaussian, $7e-4$ *rms*, truncated at 2 sigma. A random orbit of about $200 \mu\text{m}$, *rms*, appears to correlate with a 10% polarization loss through the strongest resonance, $G\gamma = 393 + Qy$. Losses across the upstream $411-Qy$ are marginal.

Appendix

A Working Hypotheses

In these simulations collision optics is used whatever the energy, for simplicity. This leans on the observation that resonance spectrum structure and strengths with injection optics do not differ much from collision optics case, in particular non-systematic resonances have similar strengths as well (as it appears, in spite of a breaking of 3-periodicity with collision optics due to β^* squeeze at IP6 and IP8).

A.1 Spin Resonance Spectrum, Intrinsic

Intrinsic resonance lines with collision optics are displayed in Fig. 2. Strengths are calculated using [1, Eq. 9.53]

$$\begin{Bmatrix} \Re(\epsilon_n^{\text{intr},\pm}) \\ \Im(\epsilon_n^{\text{intr},\pm}) \end{Bmatrix} = \frac{1+G\gamma_n}{4\pi} \sum_{\text{Qpoles}} \begin{Bmatrix} \cos(G\gamma_n\alpha_i \pm \varphi_i) \\ \sin(G\gamma_n\alpha_i \pm \varphi_i) \end{Bmatrix} (KL)_i \sqrt{\beta_{y,i} \frac{\varepsilon_y}{\pi}} \quad (1)$$

for $\varepsilon_y = 10\pi\mu\text{m}$. The envelop equation [2, Eq. 5.37]

$$\bar{S}_y = 1 - 8a^2(1-a^2), \quad a = \frac{|\epsilon_n|}{\lambda} \sin \frac{\pi\lambda}{2}, \quad \lambda = ((G\gamma - G\gamma_{\text{res.}})^2 + |\epsilon_n|^2)^{1/2} \quad (2)$$

is used for occasional checks of eigenvector tilt to the vertical across a spin resonance. \bar{S}_y is the average value of the vertical spin component in the test proton bunch. In a general manner, the agreement is good (i.e., $\bar{S}_y(G\gamma)$ from Eq. 2 matches the numerical data), if the numerical value of $|\epsilon_n|$ is taken as the resonance strength for $\approx \varepsilon_y = \text{rms beam emittance}$ - evaluated for instance from a prior Froissard-Stora crossing, snakes off [3].

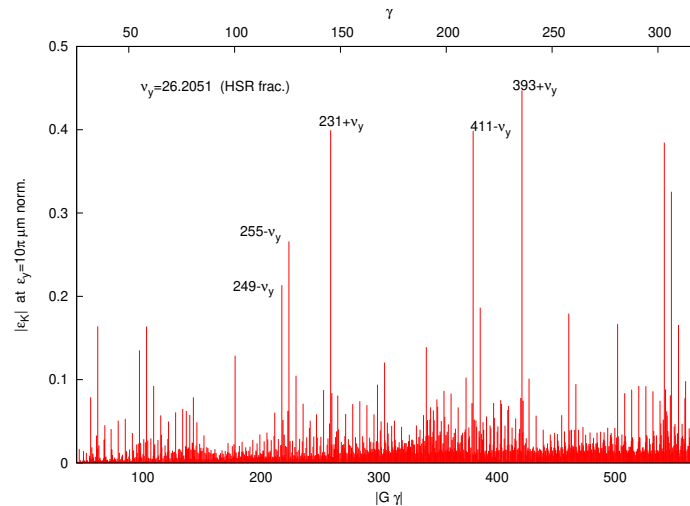


Figure 2: Strengths of intrinsic resonances, proton, store optics, nominal RHIC tunes Qx/Qy=28.685/29.673.

A.2 Spin Resonance Spectrum, Integer

Generating random dipole orbit errors in zgoubi:

```
'ERRORS'
1 1 123456
MULTIPOL(VKIC) 1 BP A U 0. 10e3 2      ! consider 10e3 a relative field scaling factor here, dimensionless
```

This introduces a random dipole field defect, Gaussian with *rms* value $\delta B = 0.6 \text{ kG}$ and 2σ cut-off, in all MULTipoles labeled VKIC. Typical resulting closed orbits, as used in these simulations, are displayed in Fig. 3. Note that a different random kicks seed (i.e., a different distribution of random kicks around the ring) may entail a substantially different *rms* closed orbit excursion.

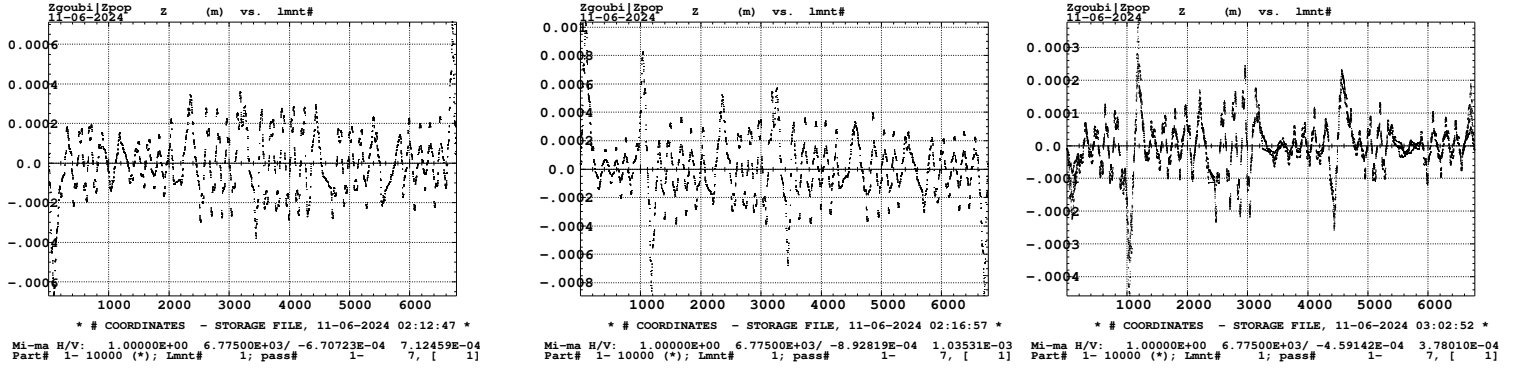


Figure 3: Vertical closed orbit for $\text{vkick}=10\text{e}3$ (arbitrary units) and different random vertical kick series around the ring. The rms closed orbit value is, left, seed 1: $160 \mu\text{m}$; center, seed 2: $241 \mu\text{m}$, right, seed 3: $82 \mu\text{m}$.

Based on the knowledge of the orbit around the ring, imperfection resonance strengths for a vertical kick series can be calculated using [1, Eq. 9.51]

$$\epsilon_n^{\text{imp}} = \frac{1 + G\gamma_n}{4\pi} \sum_{\text{Qpoles, i}} [\cos(G\gamma_n \alpha_i) + j \sin(G\gamma_n \alpha_i)] (KL)_i y_{\text{co}}(\theta_i) \quad (3)$$

That series value, ϵ_n^{imp} , may end up very different from one $y_{\text{co}}(\theta_i)$ series to another.

A.3 Spin Matrix at IP6

A sanity check: spin transfer matrix.

Case of flat orbit:

momentum group # 1:

```
-1.00000      6.158643E-06   -3.528648E-18
-6.158643E-06   -1.00000    -2.223735E-16
-3.530017E-18   -2.223735E-16      1.00000
```

Determinant = 1.00000000000
 Trace = -1.0000000000; spin precession $\text{acos}((\text{trace}-1)/2)$ = 179.9996471363 deg

Precession axis : (0.000000, 0.000000,-1.000000) -> angle to vertical is 180.0000 deg

Spin precession/2pi (or Qs, fractional) : 5.0000E-01

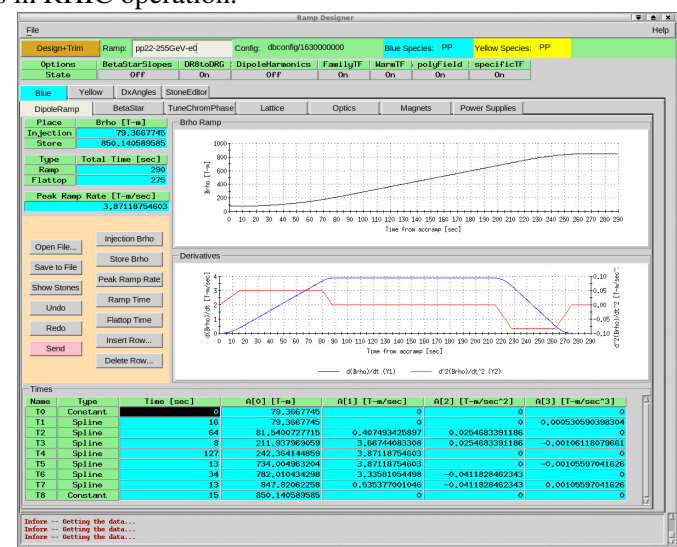
A.4 RF Settings

An acceleration $\dot{\gamma} = 1$ is taken in the simulations, the same value as in RHIC operation.

Zgoubi data are, peak voltage $\hat{V} = 68.94 \text{ kV}$, synchronous phase $\phi_s = 2.96705972839 \text{ rad}$, as follows:

```
'CAVITE' accelerating cavity data, for gamma-dot = 1
2                                ! option: Synchrotron cavity
3833.84593   360.00 ! closed orbit length; harmonic number
68.94e3  2.96705972839 ! peak voltage (V), synch. phase (rad, 170\,deg)
```

The display on the right shows actual RHIC operation data: a peak RF voltage of 33kV to 35kV in Run 22, $B\rho\text{-dot}=2$ in Yellow, 4 in Blue.



A.5 Initial Bunch; Phase-Space Motion

Particles are launched with Gaussian densities, rms emittances $\epsilon_x/\pi = \epsilon_y/\pi = 2.5 \mu\text{m}$, rms $\delta p/p = 7 \cdot 10^{-4}$.

```
'MCOBJET'
726.55d3          ! G*gamma 416.
3
1
2 2 2 2 2 2
2.53174139E-07 1.49134623E-08 1.73043964E-04 -7.82569406E-05 0. 1.
-0.144116 0.714411 11e-9 3 ! 2.5um norm
-0.043434 0.706684 11e-9 3 ! 2.5um norm
0. 80. 0.4e-4 1 ! rms length 6cm, rms dpp 7e-4
```

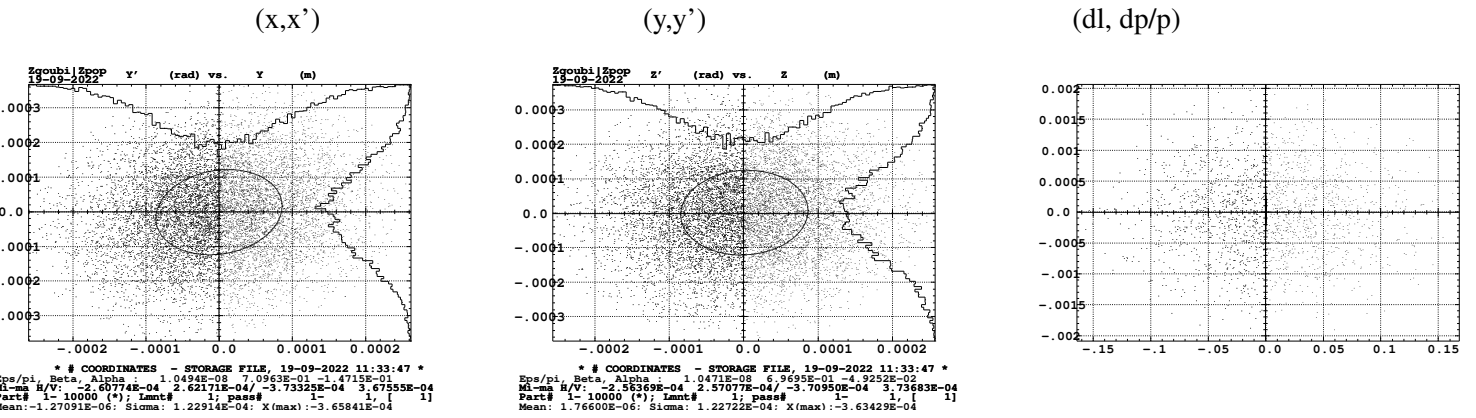


Figure 4: Initial phase spaces, at IP6. Horizontal and vertical phase spaces are matched to the lattice, longitudinal is not matched to the accelerating bucket.

Multi-turn monitoring:

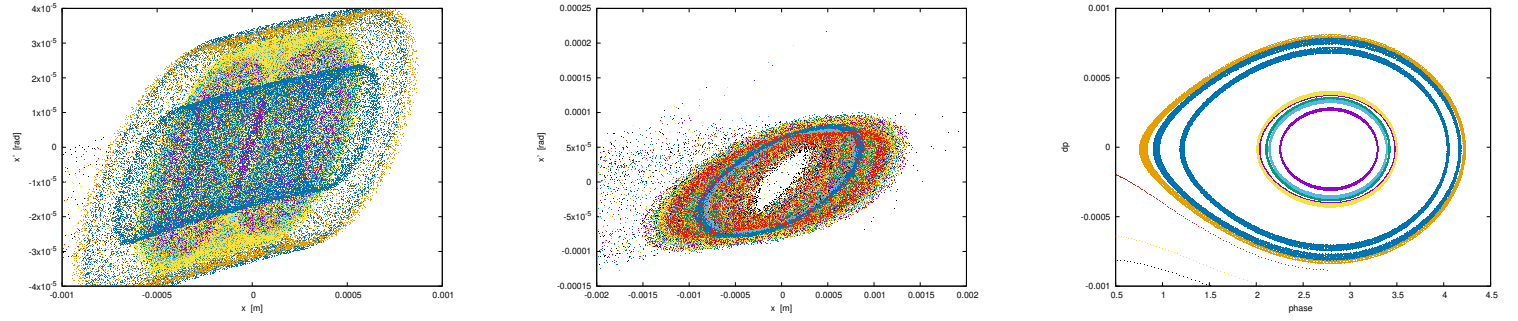


Figure 5: Monitoring: 1.2 million turn phase spaces, a few particles (different colors), observation is at 9 o'clock snake. Incidentally, a particle happens to err beyond momentum acceptance here, a few percent of the particles launched happen to be lost in that manner, after an early $\approx 100,000$ turns, in these simulations.

B Transmission Versus rms Orbit Excursion, Simulations

Simulations outcomes reported in the following may be (as indicated, for instance in Sect. B.1, case VKICK=10e3) performed with different sets of vertical dipole field defects (*i.e.* different series of kicks in the V kickers included in the lattice), which may result in different rms orbit excursion. The graphs indicate the latter.

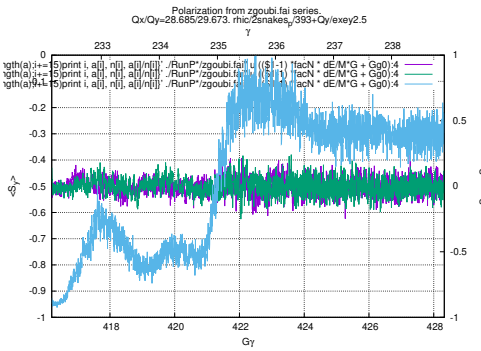
In addition, various seeds for the initial, 100+ proton, random object (MCOBJET in zgoubi's jargon) are tried.

B.1 Case 393 + Qy

Note in the case VKICK=10e3 below, the difference in closed orbit excursion (see Fig. 3, ERRORS seed 1: 160 μm vs. ERRORS seed 2: 241 μm) results in a marginal difference in polarization loss. Checking whether this is a general rule requires more statistics on ERRORS' VKICK series.

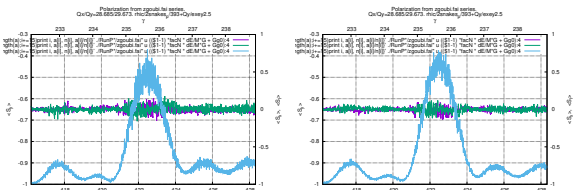
VKICK 40e3, $\sigma_y = 0.6407 \text{ mm}$

100 particles: $P_i = 940$ $P_f = .3$ $P_f/P_i = 0.3$

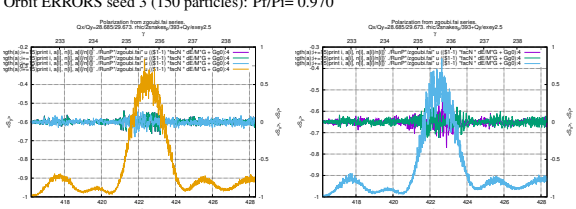


VKICK 10e3, $\sigma_y = 0.1602 \text{ mm}$

MCOBJET seed 1: $P_f/P_i = 0.950$ seed 2: $P_f/P_i = 0.971$ seed 3: $P_f/P_i = 0.970$
seeds 1+2+3 (329 particles): $\text{Pi}/\text{Pi} = 0.965$

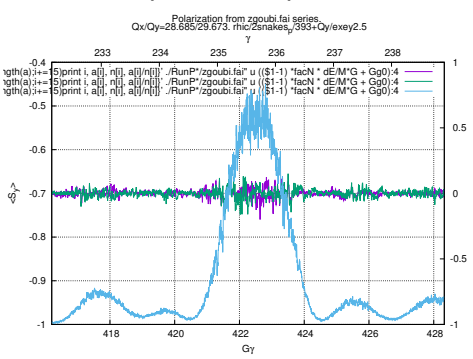


MCOBJET seed 3: $P_f/P_i = 0.970$ Orbit ERRORS seed 2 (150 particles): $\text{Pi}/\text{Pi} = 0.970$
Orbit ERRORS seed 3 (150 particles): $\text{Pi}/\text{Pi} = 0.970$



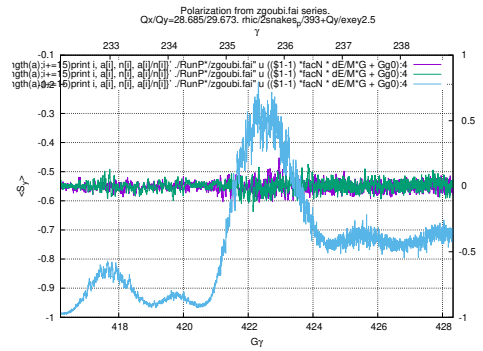
VKICK 2.5e3, $\sigma_y = 0.0400 \text{ mm}$

$P_i = -0.9958$ $P_f = -0.9910$ $P_f/P_i = 0.995$



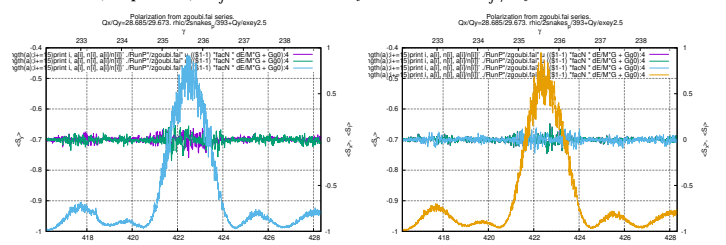
VKICK 20e3, $\sigma_y = 0.3203 \text{ mm}$

100 particles: $P_i = -0.987$ $P_f = -0.750$ $P_f/P_i = 0.760$



VKICK 5e3, $\sigma_y = 0.0801 \text{ mm}$

MCOBJET seed 1: $P_i = -0.9955$ $P_f = -0.9888$ $P_f/P_i = 0.993$
MCOBJET seed 2: $P_i = -0.9948$ $P_f = -0.9885$ $P_f/P_i = 0.994$
MCOBJET seed 3: $P_i = -0.9960$ $P_f = -0.9885$ $P_f/P_i = 0.992$
seeds 1+2+3 (277 particles): $P_i = -0.9957$ $P_f = -0.9883$ $P_f/P_i = 0.993$



Flat orbit

$P_i = -0.9957$ $P_f = -0.9920$ $P_f/P_i = 0.996$

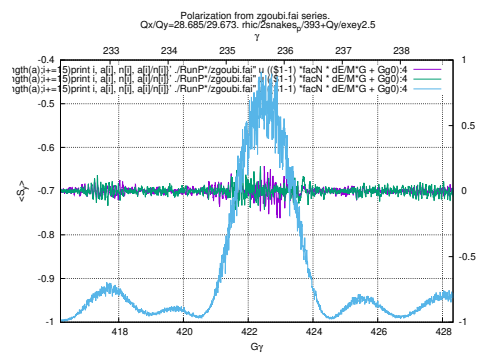
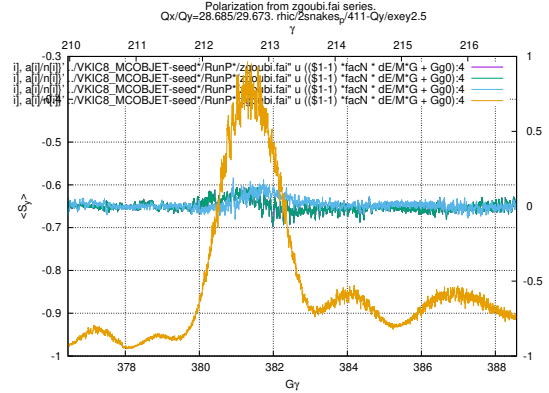


Figure 6: Crossing $G\gamma = 393 + Qy$. $\epsilon_x/\pi = \epsilon_y/\pi = 2.5 \mu\text{m}$, $\sigma_{dp/p} = 7 \cdot 10^{-4}$. Jobs of about 100 particles.

B.2 Case 411 - Qy

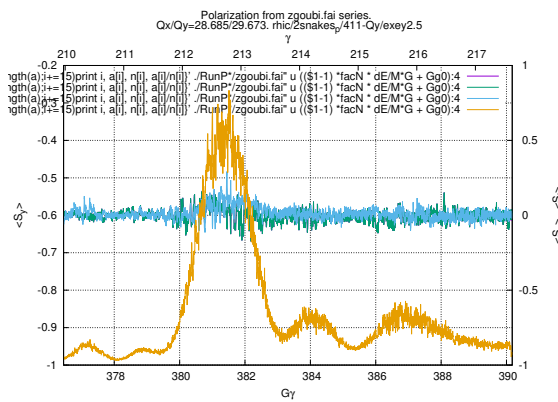
$$\sigma_y = 1.34 \text{ mm}$$

$$P_i = -0.980 \quad P_f = -0.929 \quad P_f/P_i = 0.9480$$



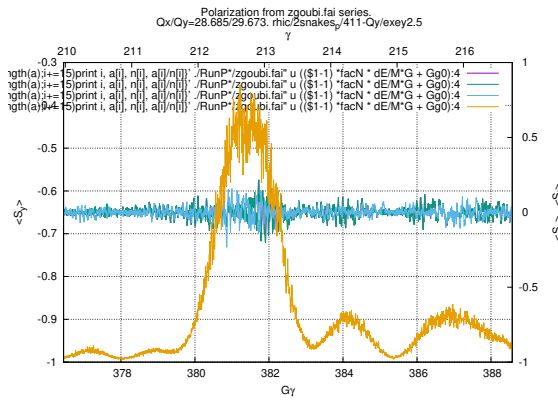
$$\sigma_y = 0.988 \text{ mm}$$

$$P_i = -0.985 \quad P_f = -0.955 \quad P_f/P_i = 0.970$$



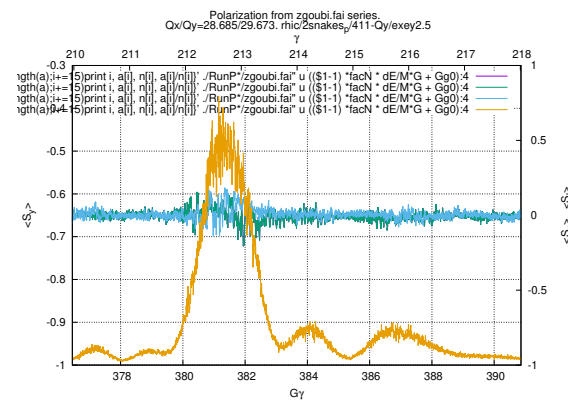
$$\sigma_y = 0.16474 \text{ mm}$$

$$P_i = -0.989 \quad P_f = -0.988 \quad P_f/P_i = 0.999$$



$$\sigma_y = 0.65 \text{ mm}$$

$$P_i = -0.989 \quad P_f = -0.985 \quad P_f/P_i = 0.996$$



$$\text{Flat orbit}$$

$$P_i = P_f = -0.990 \quad P_f/P_i = 1$$

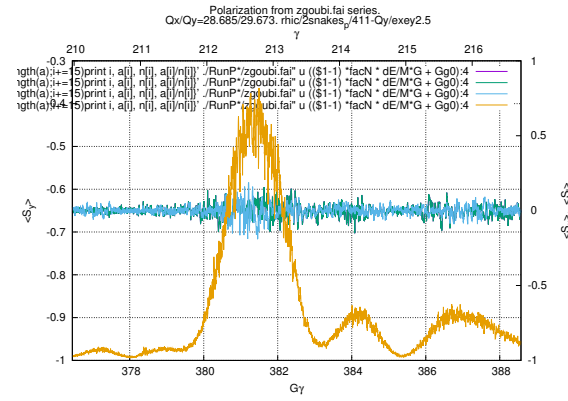


Figure 7: Crossing $G\gamma = 411 - Qy$. $\epsilon_x/\pi = \epsilon_y/\pi = 2.5 \mu\text{m}$, $\sigma_{dp/p} = 7 \cdot 10^{-4}$. Jobs of about 100 particles.

References

- [1] F. Méot: Spin dynamics. In: Polarized Beam Dynamics and Instrumentation in Particle Accelerators. Springer, 2023. <https://link.springer.com/book/10.1007/978-3-031-16715-7>
- [2] Lee, S.Y: Spin Dynamics and Snakes in Synchrotrons. World Scientific (1997)
- [3] See for instance, F. Méot: RHIC spin tracking. Spin meeting, May 2, 2012, page 15, https://www.cadops.bnl.gov/AP/SpinMeeting/2012_0502_francois.pdf